 doi:10.20944/preprints202107.0609.v1

Article

Vertical distribution of aerosols during deep-convective event in the Himalaya using WRF-Chem model at convection permitting scale.

Prashant Singh [1,2], Pradip Sarawade [1] and Bhupesh Adhikary [2,*]

[1] Department of Physics, University of Mumbai, Mumbai, India; pradip.sarawade@physics.mu.ac.in (P.S.) prashantsinghprs@gmail.com (P.S.)
[2] International Centre for Integrated Mountain Development (ICIMOD), Khumaltar G.P.O. Box 3226, Lalitpur, Nepal; Bhupesh.Adhikary@icimod.org (B.A.)

* Correspondence: Bhupesh.Adhikary@icimod.org

Abstract: The Himalayan region is facing frequent cloud burst and flood events during the summer monsoon e.g., Kedarnath flood of 2013. It was one of the most devastating event which claimed thousands of human lives, heavy infrastructure and economic losses. Fast moving monsoon, pre-existing westerlies, and orographic uplifting was reported as the major reason for cloud burst over Kedarnath in previous research. Our study illustrates the vertical distribution of aerosols during this event and its possible role using Weather Research and Forecasting model coupled with chemistry (WRF-Chem) simulations. Model performance evaluation shows that simulations can capture the spatial and temporal pattern of observed precipitation during this event. Model simulation at 25km and 4km horizontal grid resolution without any changes in physical parameterization shows very minimal average difference in precipitation. Whereas simulation at convection permitting scale shows detailed information related to parcel motion compared to coarser resolution simulation. This indicates parameterization at different resolution needs to examine for better outcome. The result shows up to 20-50% changes in rain over area near Kedarnath due to the presence of aerosols. The simulation at both resolution shows significant vertical transport of natural (increases by 50%+) and anthropogenic aerosols (increases by 200%+) during the convective event. Which leads to significant changes in cloud property, rain concentration and ice concentration in presence of aerosols. Due to aerosol–radiation feedback, the important instability indices like convective available potential energy, convective inhibition energy, vorticity etc. shows changes near Kedarnath.

Keywords: Aerosol; South Asia; WRF-Chem; Precipitation; CAPE; CIN.

1. Introduction

Dimri et al., (2017) reviewed dynamic, thermodynamic, and physical reasons of cloud burst cases in Himalayan region, and their impact to society in detail. Generally, interaction of fast-moving monsoon with existing active westerlies [2] and orographic uplifting often results havoc in the central Himalayan region [3]. Himalayan foothills make an intersection point where northward moving monsoon, active westerlies and orographic lifting produces high convection and thunderstorm activity [4]. Previous study has indicated that presence of aerosols can enhance or suppress rain over Asian region [5]. Indo Gangetic Plain (IGP) which is known as a hotspot of anthropogenic pollution in South Asia [6] as well as deserts of Rajasthan and middle east Asia [7] supply ample aerosols to Himalayan region.

Aerosol-Cloud-Precipitation interaction is considered a complex system and much remains to be understood [8–10]. Aerosols act as cloud condensation nuclei (CCN), which is necessary to form cloud and rain [8]. Some of the aerosols act as ice nuclei (IN) [11,12] which may hold the water content in clouds and delay the precipitation [13]. In the presence of excess aerosols, smaller cloud droplets are formed which reduces the precipitation amount [8]. In the form of CCN and IN in clouds, aerosols affect the cloud properties such

 doi:10.20944/preprints202107.0609.v1

as brightness, cloud cover, cloud top temperature and cloud top pressure [14–16]. Presence of aerosol layers above or below a cloud can affect the cloud cover in either way [15,16]. Andreae and Rosenfeld (2008) reported that natural aerosol and CCN concentration is lower over land and cloud formation over the continent mostly results from anthropogenic emissions. More CCN (more aerosols) leads to smaller and narrower cloud droplet size and distribution which results into suppressed warm rain and enhanced cold rain. Higher CCN in mix phased cloud makes it deeper and enhances lightning activity with more flashes [17]. Increase of 1-30% dust and sea salt concentration affect the cloud property and precipitation significantly;15% increase in dust concentration may delay rain by one hour was reported [12]. Up to 70% increase in CCN over northwestern Europe due to aged Saharan dust is reported by Bègue et al., (2015). Increased cloud fraction (~5%) and decreased cloud top pressure (~40mb) is reported due to elevated aerosol concentration over Atlantic [16]. Several studies have indicated that aerosols are not only limited to acting as CCN/IN, but that they also affect radiation derived parameters (such as convective available energy (CAPE) and convective inhibition energy (CIN) important in prediction of severe weather [10,19].

Most of the extreme precipitation events over western Himalaya are observed during the month of September based on the records available from 1875-2010 [20]. On 16th -17th June 2013, a rapid arrival of monsoon in northern India along with the presence of strong westerlies over the region was one of the major causes for a massive precipitation event over Kedarnath, India [21–24]. Kedarnath (30.73°N, 79.06°E; 3553 m from sea level) is a small town in Indian state of Uttarakhand in the Himalayan region. This study focuses on the atmospheric analysis during the Kedarnath flood which occurred during 16th - 17th June 2013, which was followed by significant flooding over western Nepal 17th - 18th June 2013, an event which was later called as Himalayan tsunami [21]. Kedarnath floods claimed loss of hundreds of human life and damaged vast infrastructure [22]. Many studies after the event tried to analyze the causes for such devastation. Some of the observation [1,22] and model [23] based studies have analyzed meteorological conditions, orographic and climatic prospective [21,25] and effect of chemistry on precipitation [5].

This study tries to understand the vertical distribution of aerosols at the synoptic and convection permitting scales during the Kedarnath heavy precipitation event using regional Weather Research Forecast coupled with chemistry (WRF-Chem) model. Model horizontal grid resolution of below 5x5km is considered as convection permitting scale where there is no need of specific cumulus parameterization schemes in the model [26,27]. Additionally, we discuss how the presence of aerosols affected radiation and altered the severe weather indices, which are important in prediction precipitation and severe weather.

2. Data and Methodology

2.1. Observations

In-situ data for various stations obtained from Meteorological & Oceanographic Satellite Data Archival Centre (MOSDAC) of Indian Space Research Organization (ISRO) containing precipitation, relative humidity, wind direction and speed, temperature and near surface pressure were used in this study. MOSDAC collects data from Indian Meteorological Department (IMD) and various Automated Weather Station (AWS) from different sources (https://www.mosdac.gov.in/).

Tropical Rainfall Measuring Mission (TRMM) monthly level 3 data (TRMM_3A12) available at horizontal grid resolution of 0.5° × 0.5° (https://disc.gsfc.nasa.gov/datacollection/TRMM_3A12_7.html) was used to analyze the general trend over the study region. Further analysis is performed using TRMM-TMPA (Multi-satellite Precipitation) level 3 data at 0.25° × 0.25° spatial resolution which was available at 3 hourly temporal resolutions.

 doi:10.20944/preprints202107.0609.v1

Atmospheric infrared sounder (AIRS) Aqua level 3 daily product available at 1° × 1° resolution (AIRX3STD) downloaded from https://search.earthdata.nasa.gov/ was used to understand the cloud property during heavy precipitation event. Moderate Resolution Imaging Spectroradiometer (MODIS) level 3 Terra (MOD08_D3) and Aqua (MYD08_D3) daily product available at 1° × 1° resolution were also used along with AIRS. Both the satellite products provided cloud fraction, cloud top pressure and temperature which were useful to understand the cloud properties.

2.2. Model Setup

Six set of simulations were performed to analyze the vertical transport of bulk aerosols during Himalayan extreme precipitation event. Out of these, three sets of WRF simulations were performed at the resolution of 25 km for the domain consisting whole Indian subcontinent (6.5˚-36.0˚N, 53.0˚-103.0˚E; Fig. S1) with MOZCART, MOZART and WRF without chemistry option. Similarly, another three sets of WRF simulation were performed at the resolution of 4 km covering area between 28˚-32.0˚N, 74.25˚-85.75˚E that covered significant portions of the IGP and Himalayas. One week spin up time was used to stabilize the chemistry in the single domain model simulations. Event analysis was carried out using the data from 3 days before to 3 days after the event. Details of the WRF simulations with MOZCART chemistry (WC25) and without chemistry at 25 km (WRF25) horizontal grid resolution and similarly at the 4 km (WC4 and WRF4 respectively) are outlined in Table 1. Thompson Graupel Scheme a double-moment microphysics scheme is used in simulations, that consist of six classes of moisture species along with number concentration of ice for prediction of cloud properties. To understand the aerosol-cloud-radiation feedback, the cloud effect to the optical depth in radiation is also activated in simulations. Supporting figure S1 shows domain of simulation at the resolution of 25 km and 4 km (red box), and location of Kedarnath (black dot).

Table 1: Domain and parameterization details for different simulations.

Simulations	WC25	WRF25	WC4	WRF4
Centered at	22˚N, 78˚E		30˚N, 80˚E	
Resolution	25x25 km		4x4 km	
No. of grids	130 x 203 x 40		223 x 555 x 40	
Domain	6.5˚-36.0˚N, 53.0˚-103.0˚E		28˚-32.0˚N, 74.25˚-85.75˚E	
Chemistry Scheme	MOZCART	-	MOZCART	-
Convective parameterization	Kain–Fritsch Scheme [1]			
Planetary boundary layer physics	Yonsei University Scheme (YSU) [2]			
Shortwave radiation physics	Dudhia Shortwave Scheme [3]			
Microphysics	Thompson graupel scheme [4]			
Longwave radiation physics	RRTM Longwave Scheme [5]			

Preprints (www.preprints.org) | NOT PEER-REVIEWED | Posted: 27 July 2021 doi:10.20944/preprints202107.0609.v1

Land-atmosphere interaction	Unified Noah Land Surface Model scheme [6]
Surface layer option	MM5 Similarity Scheme [7]
Photolysis	Madronich fast-Ultraviolet-Visible Model (F-TUV) [8]

3. Results and Discussion

3.1. Precipitation Analysis

Normal rain was reported during monsoon 2013 throughout India, except few states of India like Bihar, Arunachal Pradesh and Jammu [24], whereas June 2013 was reported with excess rain over most of the India, except north-east India [24]. Uttarakhand faced more than 191% excess rain during the month of June, which was highest compared to any other state, while overall monsoon recorded only 12% excess rain. As per IMD records, more than 13 districts of Uttarakhand recorded excess rain during June 2013 which was an unusual event in the month of June [21].

This study used TRMM monthly surface rain rate data product (TRMM_3A12) from January 1998 to December 2014 to understand the rain pattern in Uttarakhand, a state of India, and over Kedarnath, the Himalayan Mountain city. The year 2013 was a neutral year in terms of El-Niño nor La-Nina. Analysis of seasonal and annual average precipitation over Uttarakhand for the year 2013 suggested that it was an average year in terms of accumulated precipitation when compared to other years from 1998-2014. On the other hand, monthly analysis suggested that in 2013, the month of June observed highest precipitation compared to any other year. Area averaged rain rate taken from few horizontal grids over Kedarnath suggests that seasonal and annual rain rate for the year 2013 was average during the analysis period, whereas rain rate was higher compared to the state of Uttarakhand. Kedarnath grid suggests rain rate during the month of June and monsoon of 2013 was highest compared to any other year from 1998-2014 (supporting Table S1 and supporting figure S2).

Fig. 1 shows the results of 3 days accumulated rain (from 16-18 June 2013) over the simulation domain from TRMM and different versions of the WRF model. TRMM accumulated rain (Fig. 1a) shows heavy precipitation (greater than 100mm) over the western coast, northern India, Western Nepal and along with the area near to south eastern Bay of Bengal (BoB). Fig. 1b shows accumulated precipitation from the WRF WC25 simulation. The model reproduces major precipitation when compared to TRMM precipitation results, with some minor differences. Fig. 1c shows accumulated rain from WRF25 simulation which again is like TRMM observation with minor differences. Fig. 1d shows the difference in accumulated rain produced by WC25 to WRF25 simulation. The results show that precipitation is reduced in central and north-eastern part of India with chemistry option turned on. However, northern India (majorly Uttarakhand), over Arabian Sea and Bay of Bengal shows increased rain in simulation with chemistry on.

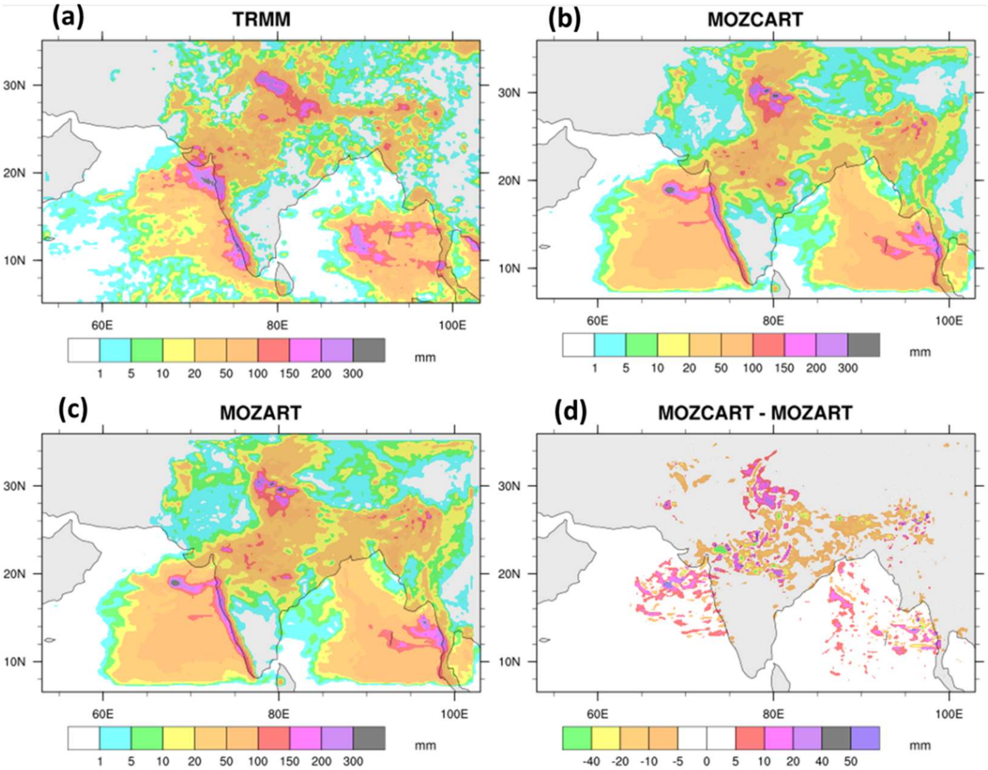

Figure 1. Three days accumulated rain from a) TRMM, and those from WRF simulations b) WC25, c) WRF25 and d) difference in rainfall between WC25 and WRF25.

Similar results are seen for the 4km resolution model simulations (Fig. 2). WRF with MOZCART chemistry (WC4) and WRF without chemistry (WRF4) show similar features of accumulated rain when compared to each other while there are differences when compared to the results obtained from TRMM. It must be noted that grid resolution between the model simulation and TRMM observation also leads to some of the observed differences. Most of the focused area of study shows decrease in precipitation from the simulations with chemistry turned on whereas few areas also show increase in precipitation. Both sets of simulations (25 km and 4 km) show effect of aerosols on precipitation amount in either direction (i.e., increase or decrease). WC25 shows most of the area over and near to Uttarakhand produces more rain in presence of aerosols while WC4 shows less rain in presence of aerosols except few concentrated places.

 doi:10.20944/preprints202107.0609.v1

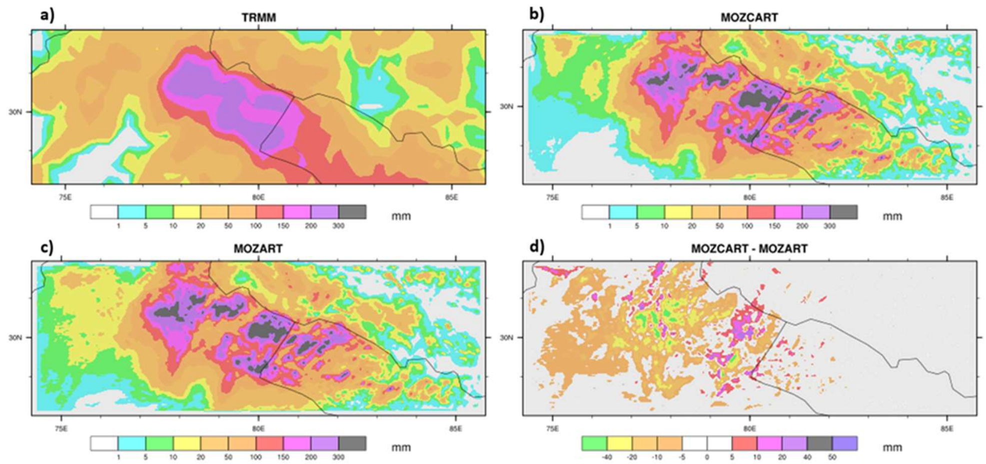

Figure 2. Three days accumulated rain from a) TRMM, and simulation of WRF at 4 km resolution b) WC4, c) WRF4 d) difference of rain produced by WC4-WRF4.

Study by Chawla et al., (2018) using combination of different parameterization schemes in WRF simulations shows that most of the combinations were able to capture spatial precipitation feature for 15th – 18th June 2013, as in TRMM with some differences. Previous study using WRF-Chem simulation by Kedia et al., (2018) suggests 20% increase in precipitation over Uttarakhand due to chemistry, using 15 days average simulated and observed rain over the region for analysis. Average precipitation and other parameters for 15 days were shown as aggregate illustrating the impact of aerosols however without providing temporal resolution for the event. Thus, it is difficult to compare our results with Kedia et al. (2018).

Fig. 3 presents time series of precipitation at four stations in Himalayan Mountains of Uttarakhand from 15th - 20th June 2013, these four-station present nearest stations to Kedarnath. In-situ observation at all four stations show that precipitation starts from morning of 16th and ends on the morning of 18th. Similar trend is observed through satellite for same time period. All four model simulations can correctly predict the start and end pattern of precipitation, and peaks in precipitation with some minor temporal shifts. At all the four stations, WC25 shows early rain whereas WRF25 shows delayed rain when compared to each other. Both WC4 and WRF4 shows delayed rain matching each other as well as matching with WRF25 simulation trend, but predict higher rainfall compared to WRF25 for the peak rain during these days. WC25 however matches the timing of the rainfall better with TRMM observations compared to other simulations.

Preprints (www.preprints.org) | NOT PEER-REVIEWED | Posted: 27 July 2021 doi:10.20944/preprints202107.0609.v1

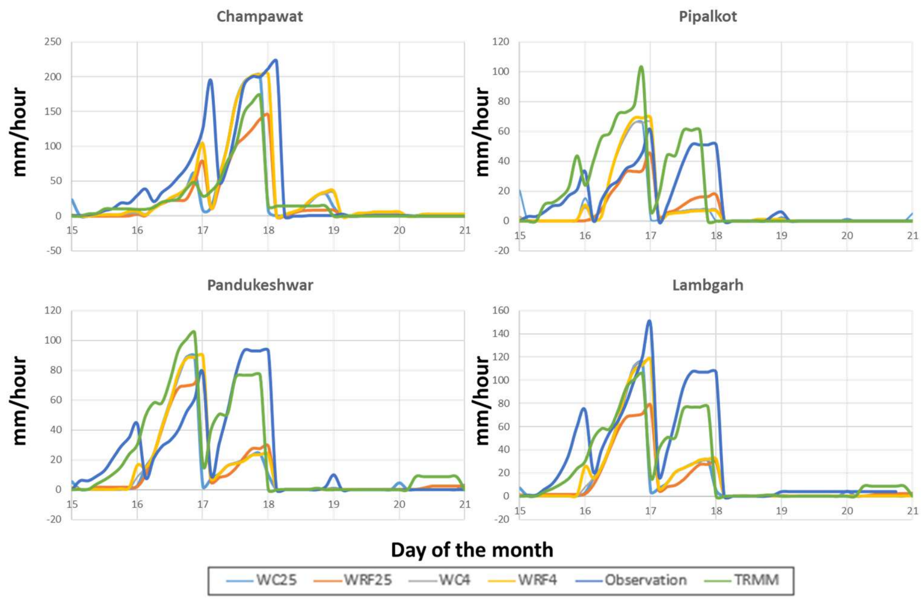

Figure 3. Precipitation from different simulation and observation from 15th - 20th June 2013 for Champawat, Pipalkoti, Pandukeshwar and Lambgarh.

Supporting Table S2, shows coefficient of determination (R2) between TRMM, in-situ observation, and all four simulations with the observations for the period from 15th – 20th June 2013. Over Kedarnath TRMM and model simulations show low value of R2 (0.36-0.41). At other places, TRMM and in-situ data shows R2 in the range of 0.32-0.60; R2 for TRMM and model ranges between 0.32-0.95 except for Dehradun. R2 between in-situ observation and model ranges between 0.23-0.93, except for Jolly Grant. R2 at Jolly Grant between TRMM and in-situ observation is 0.60, between observation and model is less than 0.31. Observed accumulated rain at Jolly Grant was high as 200 mm/day (in-situ), model produces less than 100 mm/day during event days, and model does not perform well at Dehradun station too. Over other stations model replicates the strength and period of precipitation. Observation based report from IMD presents heavy precipitation on 16th and 17th June 2013, [24] which is evident in all model simulations and satellite observations too (Fig. 3). Other observation studies also show heavy precipitation on 16th and 17th over most of Uttarakhand region [21,22,25,34].

Fig.1,2 and 3 suggest that all models simulations adequately capture the spatial and temporal coverage of precipitation, with some difference in amount of precipitation. WC25 and WRF25 show up to 50 mm/day rain difference at some of the stations, whereas WC4 and WRF4 show negligible precipitation difference. Additional analysis suggests more rain at 25 km simulation without chemistry at Dhanauri (~20 mm/day), Jolly Grant (~60 mm/day), Dehradun (~70 mm/day) and Mandal (~100 mm/day). Whereas more rain is produced at 25 km simulation with chemistry in places like Kedarnath (~40 mm/day), Champawat (~60mm/day), Nainital (~15 mm/day), Lambagrh (~40 mm/day), Pandukeshwar (~10 mm/day) and Pipalkoti (~20 mm/day). WRF and WRF-Chem were able to simulate precipitation well over most of the observation stations, which is further corroborated by TRMM observations. Given the model's ability to replicate the rainfall over Uttarakhand, we present the model-based analysis on monsoon dynamics, cloud properties and aerosols during this event.

3.2. Monsoon Dynamics

Preprints (www.preprints.org) | NOT PEER-REVIEWED | Posted: 27 July 2021 doi:10.20944/preprints202107.0609.v1

Indian Meteorological Department (IMD), India and Department of Hydrology and Meteorology (DHM), Nepal reported onset of the summer monsoon on 15th and 14th June 2013, respectively. Due to heat low (high temperature leads to low pressure zone) over northern India and high-pressure zone over adjacent ocean, moisture moves with wind from ocean to northern India during monsoon. Fig. 4a shows counterclockwise cyclonic motion of wind direction implies strong low pressure (WC25 due to full chemistry option) zone over northern India on 16th June, which guided the moisture from ocean towards the land. WC4 shows consistent winds flowing from south-east to north-west (Figure not shown). Fig. 4b shows strong low-pressure zone on 17th system, towards the north. Same low pressure zone further moved towards the western Nepal (Fig. 4d) on 18th which created flood situation in western Nepal (https://www.icimod.org/?q=10932); after 19th this system disappeared (Fig. 4e & f).

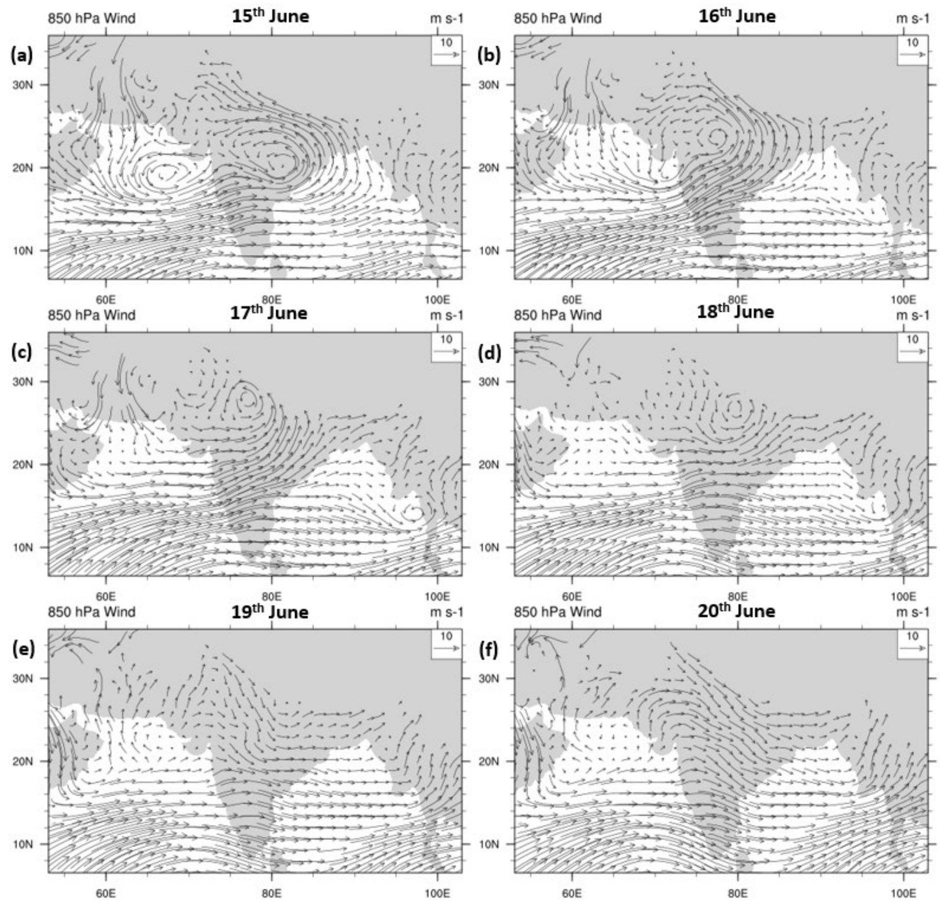

Figure 4. Daily wind speed at 850 hPa from 15th - 20th June (a-f) Simulation WC25.

Singh and Chand, (2015) had shown the presence of a low pressure zone over central India (Rajasthan and Madhya Pradesh) as simulated by their model on 16th June. Ray et al., (2014) reported presence of low-pressure system during 16th and 17th over central India. Dynamical interaction of monsoon due to low pressure system over central India with mid latitude western disturbance results into heavy rainfall [2,22,24]. Similar wind pattern and low pressure were simulated in all the simulation. Precipitation pattern is also simulated well in the simulations with respect to observation and previous literature.

Preprints (www.preprints.org) | NOT PEER-REVIEWED | Posted: 27 July 2021 doi:10.20944/preprints202107.0609.v1

In-situ observation for all stations listed in supporting table shows strong low pressure near to surface, about 4-6 hPa lesser than average atmospheric pressure on 17th. WC4 and WRF4 simulations represent better pressure at different stations in comparison to simulation WC25 and WRF25 mainly due to higher model resolution which better reflects topography height. Low pressure indicates unstable atmosphere and higher probability of precipitation. High surface relative humidity (≥90 %) was observed during 16th and 17th and the model also simulated high relative humidity for all the stations (≥ 80%). Persistent higher humidity indicates higher probability of precipitation in that area. Observation and model both show rapid decrease in relative humidity from the morning of 18th June. Observed surface temperature on 17th June at all stations fell (~ 3°-5°C) compared to average temperature. Similarly, WC25 and WRF25 shows temperature fall of ~4°-6°C while WC4 and WRF4 shows a fall of ~ 2°-6°C. All the parameters show normal atmospheric conditions from the morning of 18th June in comparison with event days. Literature based on observation shows 70-100% humidity, low pressure and low wind during event days over Kedarnath [21].

3.3. Cloud Property

Fig. 5 shows average cloud fraction (CF) from MODIS (Aqua and Terra) satellite (a-b) and average model simulated cloud fraction (c-d) for 16th and 17th June 2013. Both satellite and model show similar feature on 16th (Fig. 5a, c), dense clouds from Arabian Sea to North India passing through central India along with some dense clouds in south eastern Bay of Bengal. Both satellite and model-based observations show that all of Uttarakhand and western Nepal was covered by dense clouds on 16th. On 17th, satellite does not show dense cloud fraction over Uttarakhand and western Nepal whereas the model does simulate dense cloud fraction over area. However, on 17th, the satellite data does shows similar cloud fraction features over Western Ghats, Arabian Sea and Bay of Bengal as seen on the 16th.

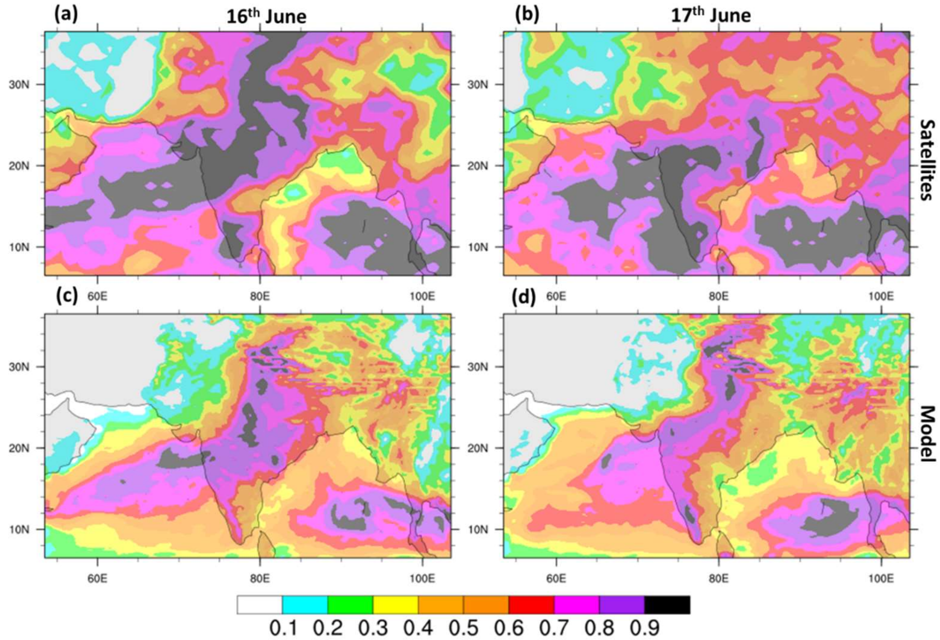

Figure 5. Average Cloud fraction on 16th and 17th June a) and b) Satellite MODIS (Aqua and Terra combined), c) and d) Model respectively.

 doi:10.20944/preprints202107.0609.v1

Model analysis reveals whole of Arabian Sea, Bay of Bengal and central India is covered with low and mid-level clouds (Figure not shown). In this study low cloud is consider up to 800 hPa, mid-cloud below 450 hPa and high cloud above 450 hPa. Along with low and mid-level clouds, Uttarakhand, Western Nepal, small part in Arabian Sea and Bay of Bengal was covered with dense high-level clouds on 16th and 17th June. Satellite observed low cloud top pressure (CTP) over Uttarakhand compared to surrounding areas (~300 hPa) on 16th and (~400 hPa) on 17th, indicating presence of high-level cloud over Uttarakhand.

Low cloud top temperature (CTT) was observed from satellite (~ -30°C to -40°C) on 16th and (~ -20°C to -30°C) on 17th over Uttarakhand and Western Nepal. CTT from model simulation was lower in comparison with surrounding over Uttarakhand and western Nepal (~-10°C to -20°C) on both days. WC4 simulates further cooler CTT on 17th (~ -30°C to -40°C). Presence of aerosol mostly produces warmer cloud top at WC25 except some places near to Kedarnath, WC4 simulated changes in CTT variation (± 15°C). Lower CTP and CTT indicates the deep cloud with high amount of precipitation [13].

At 25 km resolution, presence of aerosols affects cloud fraction by ±25% away from the major sources of emission (inferred from Fig. 1d). Presence of aerosols simulated more cloud at low level whereas decrease in the high-level clouds, while the mid-level clouds get affected in both ways over the domain of simulation. Similar results were simulated at 4 km resolution with and without aerosols for both days. The presence of aerosols played a role in creating warm clouds at central and eastern parts of India, the same region where aerosols affected precipitation negatively (Fig. 1d). Satellite data along with model shows low CTT and CTP over Kedarnath during 16th and 17th compare to previous days. Model indicates presence of dense high cloud over Kedarnath which could result in a heavy downpour.

3.4. Aerosol Concentration

Satellite and model analysis suggests presence of dense high-level (above 6 km) clouds over Kedarnath, so we analyzed aerosols above 6 km (above ~500 hPa). Our results show that over Kedarnath, there is an elevated concentration of anthropogenic and natural aerosols at high altitude during the event days. Fig. 6a-b shows area average concentration of black carbon (BC) over Uttarakhand (~29°-31°N, ~78°-81°E) from 15th - 19th. Night of 17th shows highest BC concentration at 500 hPa (> 0.25 μg/m3) and above in WC25 whereas it was (> 0.05 μg/m3) in WC4 simulations, columnar average BC concentration was higher by ~0.1 μg/m3 in WC25 whereas it was lower in WC4 from previous day. Fig. 3 shows precipitation peak was present for similar period over most of the stations. Similarly natural aerosol Dust shows higher concentration at 500 hPa and above in the both simulations WC4 and WC25 (Fig. 4c-d).

Preprints (www.preprints.org) | NOT PEER-REVIEWED | Posted: 27 July 2021 doi:10.20944/preprints202107.0609.v1

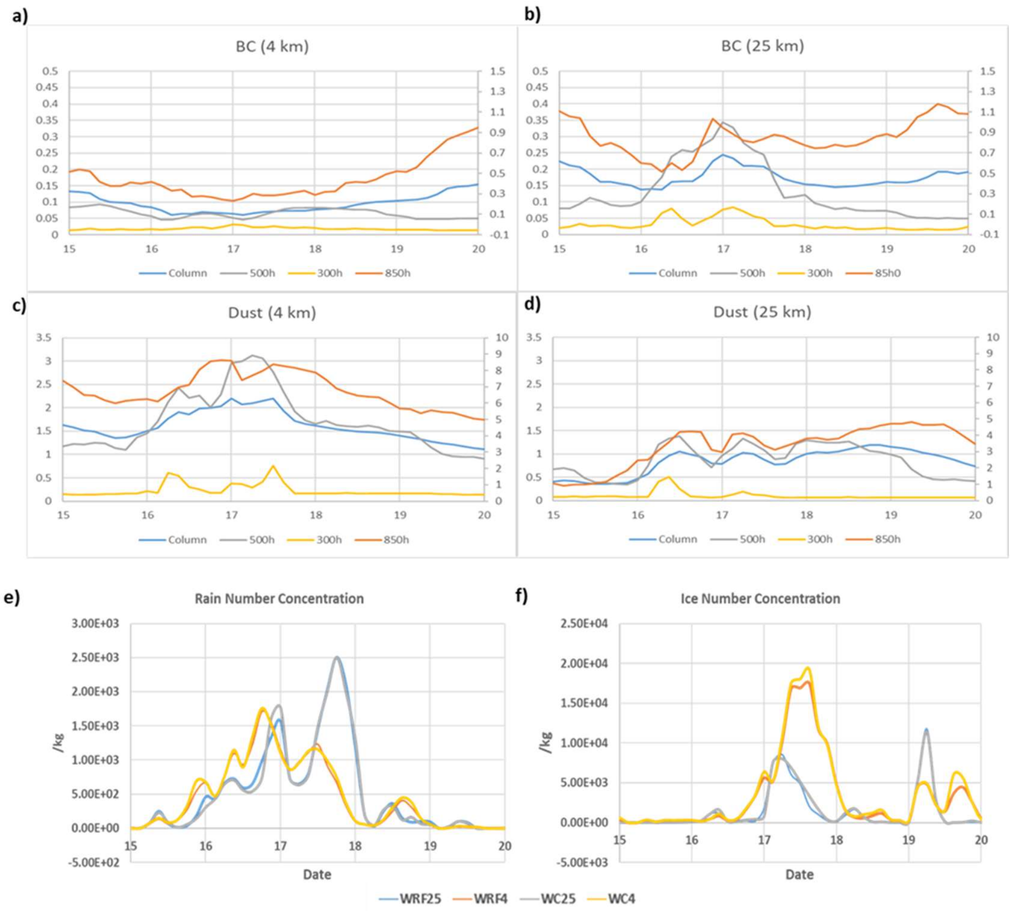

Figure 6. (a-b) BC concentration from 15th - 19th June 2013 at 850 hPa, 500 hPa, 300 hPa and columnar average at 4km and 25 km resolution, (c-d) for Dust. (e) Rain number and (f) ice number concentration with different model simulations.

Other bulk aerosol species like organic carbon (OC), dust (different size), sea salt (different size) and sulfate shows similar elevated peaks at 500 hPa and above. Table 2 presents difference in concentration of various aerosol species at 850 hPa, 500 hPa, 3 hPa and total column average. The methodology of calculating the difference in concentration is as follows:

For any aerosol species X (BC, OC, dust (all size), sea Salt (all size), sulfate), ΔX=Area Average concentration (average (Non Precipitation dates))- Area Average concentration (average (Precipitation date)) ………… (1)

X= Column,850 hPa,500 hPa or 300 hPa

Non Precipitating dates=15th ,18th ,19th and 20th

Precipitation date=16th or 17th

Area Average over Uttarakhand (~29°-31°N,~78°-81°E)

Table 2: Δconcentration for different aerosols and Δ in absolute percentage in model column and at 850 hPa, 500 hPa, 300 hPa for 16th and 17th June 2013 over Kedarnath at 25km resolution.

Aerosols	16th June 2013							
	Δ Column		Δ 850 hPa		Δ 500 hPa		Δ 300 hPa	
	ug/m3	%	ug/m3	%	ug/m3	%	ug/m3	%
BC	-0.001	-0.56	-0.225	-25.10	0.156	200.26	0.029	142.23
OC	-0.023	-2.15	-1.672	-28.86	1.038	226.53	0.177	240.49
DUST1	0.685	36.86	2.409	40.01	1.124	45.43	0.352	95.92
DUST2	1.264	29.56	4.893	34.38	2.069	38.09	0.775	104.79
DUST3	0.766	26.03	3.189	30.91	1.384	40.55	0.549	137.52
DUST4	-0.054	-5.85	-0.764	-17.66	0.357	50.64	0.149	230.30
DUST5	-0.031	-47.90	-0.165	-57.98	-0.027	-39.57	0.003	19.12
SEA SALT1	0.008	93.74	0.026	71.09	0.015	210.09	0.002	41.50
SEA SALT2	0.075	128.65	0.22	71.48	0.146	493.88	0.021	1478.02
SEA SALT3	0.058	152.67	0.194	87.73	0.083	540.52	0.011	3580.23
SEA SALT4	0.0002	873.93	0.0011	653.67	0.0001	1481.69	0.00001	43480.71
sulf	-0.028	-2.82	-1.349	-28.99	0.711	85.37	0.126	72.73

 doi:10.20944/preprints202107.0609.v1

	17th June 2013							
	Δ Column		Δ 850 hPa		Δ 500 hPa		Δ 300 hPa	
	ug/m3	%	ug/m3	%	ug/m3	%	ug/m3	%
BC	0.03	20.82	-0.039	-4.36	0.154	197.75	0.031	151.07
OC	0.189	17.89	-0.473	-8.17	0.981	214.08	0.152	205.95
DUST1	0.298	16.05	1.412	23.44	0.489	19.75	0.108	29.43
DUST2	0.615	14.37	3.033	21.31	1.212	22.31	0.227	30.63
DUST3	0.423	14.38	2.063	20.00	0.999	29.29	0.148	37.05
DUST4	-0.043	-4.62	-0.773	-17.85	0.387	54.91	0.042	64.18
DUST5	-0.025	-38.44	-0.137	-48.18	-0.012	-17.96	0.001	-7.58
SEA SALT1	0.008	93.29	0.031	86.71	0.011	148.71	0.001	9.00
SEA SALT2	0.077	132.31	0.284	91.95	0.107	362.54	0.009	690.37
SEA SALT3	0.036	95.69	0.137	61.89	0.047	307.40	0.004	1261.94
SEA SALT4	0.0001	220.35	0.0002	122.56	0.00003	291.73	0.000002	7656.47
sulf	-0.056	-5.60	-1.087	-23.37	0.405	48.55	0.073	41.89

Most of the bulk aerosol species BC, OC, dust and sea salt shows elevated concentration at 850 hPa and above specially at higher elevation of 500 hPa. DUST5 decreases while Sea Salt4 and Sea Salt1 increase insignificantly on 16th and 17th at all

 doi:10.20944/preprints202107.0609.v1

elevations. Near surface (850 hPa) concentration of DUST4, BC and OC decreases during heavy precipitation events. At 500 hPa and above, BC, OC, Dust2, 3, 4 and Sea Salt2, 3 increases significantly during the precipitation event days. Sulfate concentration was less in column and near surface, whereas at 500 hPa and above concentration was significantly higher during 16^{th} – 17^{th} (Table 2). Similar results are observed with 4km resolution simulation (Supporting Table S3) with lower ratio of concentration in vertical layers compare to 25km resolution.

Further analysis at 500 hPa and above suggest bulk aerosols follow the fast moving moisture content from 15^{th} of June from easter coast of India to Himalayan region till 18^{th} June. The concenration of aerosols were much higher than the stable atmospheric condition in that region. Study suggest significant uplifting of aeosols in mid-troposphere during deep convective events as suggested in previous study [36]. Supporting Figure S3a shows lesser concentration of BC near surface (850 hpa) during the event period, whereas Supporting Figure S3b and S3c shows significant amount of BC over 500 hPa and 300 hPa in the active convective area during the event. Other earosols also shows similar feature in the free troposphere. That indicate strong vertical transport of aerosols during the strong convective events over the effective region, which is evident in BC flow analysis in Supporting Figure S4a and S4b. Those figure shows strong updraft of BC from the plains towards to Hiamalyan region during the event day. With convection anthropogenic and natural aerosols transport significantly above 500 hPa and above, which further transported through synoptic monsoon motion in atmosphere.

Aerosols act as IN and CCN, responsible for creating clouds and precipitation [11,12]. Model analysis of average columnar rain number concentration (RNC) and ice number concentration (ICC) over Kedarnath (Fig. 6 e-f), reveal elevated concentration of RNC during 16^{th} and 17^{th} June while ICC shows elevated concentration on the 17^{th} and a smaller peak on the 19^{th}. While there is significant difference between model simulations at 25 km and 4 km resolution, there is minimal difference when taking chemistry (i.e., aerosols) into account. On 16^{th}, all models simulated good number of RNC whereas ICC was not significantly high over Kedarnath. Higher RNC delays the precipitation time, which leads to higher and deeper clouds [17] as observed by satellite and model over Kedarnath on the 16^{th} (Fig. 5a-b).

On 17^{th} June, above 500 hPa, significantly high amount of ICC was present (figure not shown), which justifies cooler cloud top, as observed by satellites over Kedarnath. RNC, ICC (Fig. 6e-f) and precipitation (Fig. 3) patterns suggest two events. First event (peak) before 17th, which was continuously increasing from the evening of 15th to 16th that resulted into downpour at late night of 16^{th} – 17^{th}. Second event with RNC and ICC peak values that was present during daytime of 17^{th}, leads to precipitation on late evening but with lesser quantity. Our results suggest that high amount of ICC held the precipitation within cloud which then moved with the synoptic circulation towards western Nepal on 18th, resulting into heavy downpour there.

Analysis of extinction coefficient profile from WC25 and WRF25 show higher difference in extinction coefficient between the heights 2 to 8 km (calculated from equation 1) whereas RNC significantly increases in presence of aerosols at 4-6 km on both days over Kedarnath. During both days ICC decreases significantly in the presence of aerosols. Supporting Fig S5 and S6 shows decreased ICC above 6km during 16th and 17th. Satellites were not able to capture aerosol optical depth (AOD) during event day, even nearby AERONET station (over Kanpur) doesn't have data, therefore AOD comparison with observation was not possible. On 17^{th} CALIPSO shows 3% of data availability, data loss reported due to a ground station anomaly (https://www-

Preprints (www.preprints.org) | NOT PEER-REVIEWED | Posted: 27 July 2021 doi:10.20944/preprints202107.0609.v1

calipso.larc.nasa.gov/products/lidar/browse_images/data_event_log.php?s=production&v=V3-30&browse_date=2013-06-17), whereas 16th and 18th passes were far from the area of interest.

Analysi suggest, presence of anthropogenic and natural aerosols (BC, OC, Dust, sulfate and Sea Salt) in free troposphere above 2 km leads to increase in RNC which results in more precipitation over Kedarnath region. Result shows higher concentration of aerosols at elevated layers affected the ICC numbers negatively which resulted into more precipitation into region. Aerosols over the simulation domain affected the cloud and precipitation in either way.

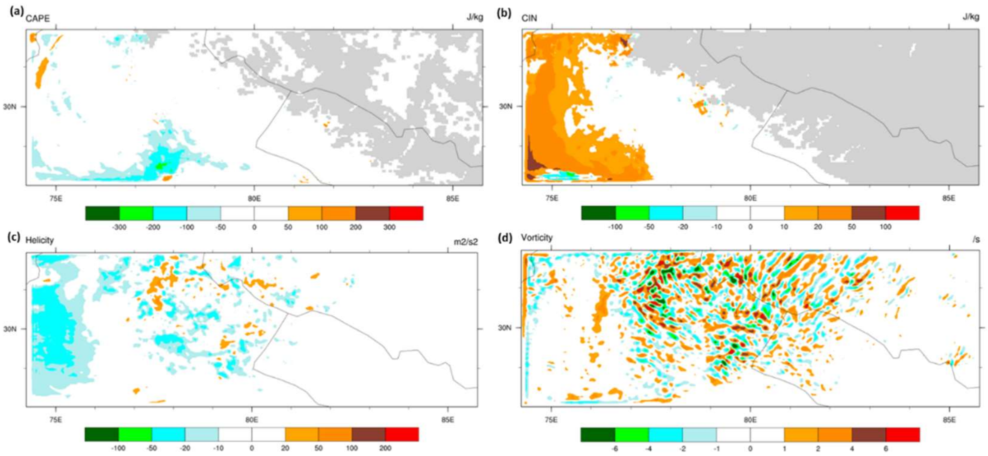

Figure 7. Effect of aerosols on a) CAPE, b) CIN, c) helicity and d) vorticity at 4 km resolution (WC4-WRF4) during 17th June.

We also considered to evaluate the parameters that are important to indicate severe weather such as Convective Available Potential Energy (CAPE), convective inhibition energy (CIN), vorticity and helicity [37,38]. CAPE was simulated high (≥1000 J/kg) over BoB, Arabian Sea and many parts of Indian subcontinent in WC25, whereas Kedarnath region doesn't show high CAPE values during the event days. CIN was very less (≤50 J/kg) over most of the area except over Pakistan and Northern India (≥ 100 J/kg), during event days. Strong (≥ 12 10^(-5)/s) vorticity is simulated in models along the low-pressure zone (Fig. 3). Strong helicity (≥ 400 m2/s2) also simulated over Arabian Sea and over Uttarakhand. Presence of aerosols affects the radiation over the region which results into changes on above parameters. At 25 km and 4 km, presence of aerosols shows (≥± 300 J/kg) changes in CAPE, (≥± 50 J/kg) CIN, (≥± 100 m2/s2) helicity, and (≥± 6 *10^(-5)/s) vorticity values over many part in the domain of simulation. Over Uttarakhand, presence of aerosols increased ~200 J/kg in CAPE, ~20 J/kg in CIN, up to 100 m2/s2 in helicity and above 4 * 10^{-5}/s in vorticity.

At 4 km simulation aerosols effect shows up to ± 200 J/kg changes in value of CAPE at the event day in the domain of simulation. (Fig. 7a), CIN values significantly affected by presence of aerosols. Whereas similar results are simulated at 25 km resolution simulation (Supporting figure 7a, b). Helicity and vorticity show strong variation in presence of aerosols over Kedarnath and nearby area at convection permitting scale (Fig. 7c, d). Helicity and vorticity changes are not very evident at 25 km resolution (Supporting figure 5c, d). At convection permitting scale variation in the parameters affected by orographic and thermodynamic are more evident than at low resolution simulations.

 doi:10.20944/preprints202107.0609.v1

Results indicate that the presence of aerosol does not only affect cloud and precipitation by acting as CCN and IN but also affects the severe weather indices; CAPE, CIN, helicity and vorticity show significant changes in presence of aerosols. Over the Uttarakhand and near to Himalayan foothills, CAPE, CIN, helicity and vorticity significantly increases in presence of aerosols.

4. Summary and Conclusions

Long term (1998-2014) analysis of precipitation from TRMM over Kedarnath suggested that heavy precipitation during month of June over Kedarnath is unusual event. Analysis shows June of 2013 experienced highest precipitation compared to June month of any other year from 1998-2014, otherwise year 2013 was recorded as normal monsoon year. We used six sets of model simulations at 25 km and 4 km resolution (three each), and further analysis was done using four sets of simulations (two from each resolution). We dropped two sets of simulations (one from each resolution), since chemistry without aerosols (MOZART) and without chemistry shows no significant difference in precipitation amount at both resolutions.

All model simulations captured TRMM observed spatial coverage of precipitation with some differences. Presence of aerosols shows significant increase in precipitation over Kedarnath and nearby area, whereas suppressed precipitation over central and eastern part of India was observed at 25 km resolution. Aerosols at convection permitting scale (4 km resolution) shows similar results with more regional variation and differences in precipitation changes due to presence of aerosols. In situ observations and TRMM data over many stations near to Kedarnath shows that model capture temporal trend and strength of precipitation with some differences. Model captured the consistent movement of low-pressure system from central India on 16th to Kedarnath on 17th and further towards western Nepal on 18th, as reported in literature, while it dissipated on 19th. Temperature, pressure, and humidity are also well replicated by model with observation. Cloud properties such as cloud fraction, cloud top temperature and pressure is also well simulated by model as observed from satellite.

Model simulation shows deep clouds (above 500 hPa) over Kedarnath and some other parts over ocean on 16th and 17th. Model analysis suggested presence of aerosols above 500 hPa which may act as CCN/IC. High amount of RNC and ICC over Kedarnath on 16th and 17th suggest the role of aerosols in heavy precipitation event over Kedarnath. Some the stations showed 100 mm/day increase in rain due to presence of aerosols, most of the stations showed ~±40 mm/day difference. Average profile analysis shows unusual presence of aerosols over Kedarnath and significant changes in rain and ice concentration number in presence of aerosols. The effect of aerosols on precipitation was not only limited to CCN and IN in clouds, aerosol-radiation feedback makes significant alteration in precipitation. Analysis of CAPE, CIN, vorticity and helicity show positive feedback of radiation in the region where precipitation was high and negative effect on the area where precipitation was less (Fig. 1d). Himalayan orographic lifting, fast moving monsoon due to low pressure generated from 15th – 18th June 2013, active westerlies, and aerosols effect on cloud formation due to direct as CCN/IN and indirect radiative effect made this event so devastating. Further detailed analysis of such system is necessary to understand vertical transport of aerosols and its' effect on cloud properties and convection dynamics in the Himalayan region.

Supplementary Materials: The following are available online at www.mdpi.com/xxx/s1, Figure S1: Domain of simulation at 25 km resolution, domain of simulation at 4 km resolution (red box) and Kedarnath (black dot)., Figure S2: Rain rate over Uttarakhand, nearby Kedarnath and over Kedarnath average for annual, monsoon and June month., Figure S3: Difference of Extinction Coefficient, rain and ice concentration profile over Kedarnath during a) 16th June and b) 17th June from WC25, WRF25 simulations., Figure S4: Difference of Extinction Coefficient, rain and ice concentration profiles over Kedarnath during a) 16th June and b) 17th June from WC4, WRF4 simulations (WC4-WRF4)., Figure S5: Effect of aerosols on a) CAPE, b) CIN, c) helicity and d) vorticity at 25 km resolution (WC25-WRF25) during 17th June., Figure S6a: BC1 concentration at 850 hPa from 14th - 19th June 2013., Figure S6b: BC1 concentration at 500 hPa from 14th - 19th June 2013., Figure S6c: BC1 concentration at 300 hPa from 14th - 19th June 2013., Figure S7a: BC1 volume flow on 17th June 2013, 25 km resolution (gif)., Figure S7b: BC1 volume flow on 17th June 2013, 4 km resolution (gif)., Table S1: Average rain rate (mm/hr) over Uttarakhand, Kedarnath and nearby area for the period of 1998-2014 from TRMM., Table S2: R^2 of precipitation from different simulation with observed precipitation from in situ and satellite observation., Table S3: Δconcentration for different aerosols and Δ in absolute percentage in model column and at 850 hPa, 500 hPa, 300 hPa for 16th and 17th June 2013 over Kedarnath at 4km resolution.

Author Contributions: Data curation, P.S., and B.A.; Formal analysis, P.S., P.S. and B.A.; Writing—original draft, P.S. and B.A.; Writing—review & editing, P.S., P.S. and B.A.

Funding: Not applicable.

Institutional Review Board Statement: Not applicable.

Informed Consent Statement: Not applicable.
Data Availability Statement: Most of the publicly available data website link is provided in respective places. For model data interested one may contact corresponding author through email.

Acknowledgments: This study was partially supported by core funds of ICIMOD contributed by the governments of Afghanistan, Australia, Austria, Bangladesh, Bhutan, China, India, Myanmar, Nepal, Norway, Pakistan, Sweden, and Switzerland.

Authors want to acknowledge observational data used in this study is provided by MOSDAC, SAC, ISRO.

Conflicts of Interest: The authors declare no conflict of interest.

References

1. Dimri, A.P.; Chevuturi, A.; Niyogi, D.; Thayyen, R.J.; Ray, K.; Tripathi, S.N.; Pandey, A.K.; Mohanty, U.C. Cloudbursts in Indian Himalayas: A review. Earth-Science Rev. 2017, 168, 1–23, doi:10.1016/j.earscirev.2017.03.006.
2. Sikka, D.R. SYNOPTIC AND MESO-SCALE WEATHER DISTURBANCES OVER SOUTH ASIA DURING THE SOUTHWEST SUMMER MONSOON SEASON; Chang, C.-P., Ding, Y., Lau, N.-C., Johnson, R.H., Wang, B., Yasunari, T., Eds.; 2nd ed.; World Scientific, 2010; ISBN 9789814343404.
3. Das, S.; Ashrit, R.; Moncrieff, M.W. Simulation of a Himalayan cloudburst event. J. Earth Syst. Sci. 2006, 115, 299–313, doi:10.1007/BF02702044.
4. Lau, W.K.M.; Kim, K.M.; Shi, J.J.; Matsui, T.; Chin, M.; Tan, Q.; Peters-Lidard, C.; Tao, W.K. Impacts of aerosol–monsoon interaction on rainfall and circulation over Northern India and the Himalaya Foothills. Clim. Dyn. 2017, 49, 1945–1960, doi:10.1007/s00382-016-3430-y.
5. Kedia, S.; Vellore, R.K.; Islam, S.; Kaginalkar, A. A study of Himalayan extreme rainfall events using WRF-Chem. Meteorol. Atmos. Phys. 2018, doi:10.1007/s00703-018-0626-1.
6. Gautam, R.; Hsu, N.C.; Lau, K.M.; Tsay, S.C.; Kafatos, M. Enhanced pre-monsoon warming over the Himalayan-Gangetic region from 1979 to 2007. Geophys. Res. Lett. 2009, 36, doi:10.1029/2009GL037641.
7. Seinfeld, J.H.; Carmichael, G.R.; Arimoto, R.; Conant, W.C.; Brechtel, F.J.; Bates, T.S.; Cahill, T.A.; Clarke, A.D.; Doherty, S.J.; Flatau, P.J.; et al. ACE-ASIA: Regional climatic and atmospheric chemical effects of Asian dust and pollution. Bull. Am. Meteorol. Soc. 2004, 85, 367–380, doi:10.1175/BAMS-85-3-367.
8. Devara, P.C.S.; Manoj, M.G. Aerosol-cloud-precipitation interactions: A challenging problem in regional environment and climate research. Particuology 2013, 11, 25–33, doi:10.1016/j.partic.2012.07.006.
9. Lebo, Z.J.; Feingold, G. On the relationship between responses in cloud water and precipitation to changes in aerosol. Atmos. Chem. Phys. 2014, 14, 11817–11831, doi:10.5194/acp-14-11817-2014.
10. Stevens, B.; Feingold, G. Untangling aerosol effects on clouds and precipitation in a buffered system. Nature 2009, 461, 607–613, doi:10.1038/nature08281.
11. Andreae, M.O.; Rosenfeld, D. Aerosol-cloud-precipitation interactions. Part 1. The nature and sources of cloud-active aerosols. Earth-Science Rev. 2008, 89, 13–41, doi:10.1016/j.earscirev.2008.03.001.

Preprints (www.preprints.org) | NOT PEER-REVIEWED | Posted: 27 July 2021 doi:10.20944/preprints202107.0609.v1

12. Solomos, S.; Kallos, G.; Kushta, J.; Astitha, M.; Tremback, C.; Nenes, A.; Levin, Z. An integrated modeling study on the effects of mineral dust and sea salt particles on clouds and precipitation. Atmos. Chem. Phys. 2011, 11, 873–892, doi:10.5194/acp-11-873-2011.
13. Lin, J.C.; Matsui, T.; Pielke, S.A.; Kummerow, C. Effects of biomass-burning-derived aerosols on precipitations and clouds in the Amazon Basin: A satellite-based empirical study. J. Geophys. Res. Atmos. 2006, 111, doi:10.1029/2005JD006884.
14. Bond, T.C.; Doherty, S.J.; Fahey, D.W.; Forster, P.M.; Berntsen, T.; Deangelo, B.J.; Flanner, M.G.; Ghan, S.; Kärcher, B.; Koch, D.; et al. Bounding the role of black carbon in the climate system: A scientific assessment. J. Geophys. Res. Atmos. 2013, 118, 5380–5552, doi:10.1002/jgrd.50171.
15. Khain, A.; Rosenfeld, D.; Pokrovsky, A. Aerosol impact on the dynamics and microphysics of deep convective clouds. Q. J. R. Meteorol. Soc. 2005, 131, 2639–2663, doi:10.1256/qj.04.62.
16. Koren, I.; Kaufman, Y.J.; Rosenfeld, D.; Remer, L.A.; Rudich, Y. Aerosol invigoration and restructuring of Atlantic convective clouds. Geophys. Res. Lett. 2005, 32, 1–4, doi:10.1029/2005GL023187.
17. Tao, W.K.; Chen, J.-P.; Li, Z.; Wang, C.; Zhang, C. IMPACT OF AEROSOLS ON CONVECTIVE CLOUDS AND PRECIPITATION. Rev. Geophys. 2012, 50, 1–62, doi:10.1029/2011RG000369.1.INTRODUCTION.
18. Bègue, N.; Tulet, P.; Pelon, J.; Aouizerats, B.; Berger, A.; Schwarzenboeck, A. Aerosol processing and CCN formation of an intense Saharan dust plume during the EUCAARI 2008 campaign. Atmos. Chem. Phys. 2015, 15, 3497–3516, doi:10.5194/acp-15-3497-2015.
19. Rosenfeld, D.; Lohmann, U.; Raga, G.B.; O'Dowd, C.D.; Kulmala, M.; Fuzzi, S.; Reissell, A.; Andreae, M.O. Flood or Drought : How Do Aerosols Affect Precipitation ? Science (80-.). 2008, 321, 1309–1313, doi:10.1126/science.1160606.
20. Nandargi, S.; Dhar, O.N. Extreme Rainstorm Events over the Northwest Himalayas during 1875–2010. J. Hydrometeorol. 2012, 13, 1383–1388, doi:10.1175/jhm-d-12-08.1.
21. Singh, R.; Siingh, D.; Gokani, S.A.; Buchunde, P.S.; Singh, R.P.; Singh, A.K. Brief Communication: Climate, topographical and meteorological investigation of the 16–17 June 2013 Kedarnath (India) disaster causes. Nat. Hazards Earth Syst. Sci. Discuss. 2015, 3, 941–953, doi:10.5194/nhessd-3-941-2015.
22. Singh, C.; Chand, R. Exceptionally heavy rainfall over Uttarakhand during 15-18 June, 2013 - A case study. Mausam 2015, 66, 741–750.
23. Chawla, I.; Osuri, K.K.; Mujumdar, P.P.; Niyogi, D. Assessment of the Weather Research and Forecasting (WRF) model for simulation of extreme rainfall events in the upper Ganga Basin. Hydrol. Earth Syst. Sci. 2018, 22, 1095–1117, doi:10.5194/hess-22-1095-2018.
24. Ray, K.; Bhan, S.C.; Sunitha Devi, S. A METEOROLOGICAL ANALYSIS OF VERY HEAVY RAINFALL EVENT OVER UTTARAKHAND DURING 14-17 JUNE, 2013. Imd 2014, 37–54.
25. Shukla, D.P.; Dubey, C.S.; Usham, A.L. Orographic Control of the Kedarnath disaster Orographic control of the Kedarnath disaster. Curr. Sci. 2013, 105, 1474–1476.
26. Satoh, M.; Tomita, H.; Miura, H.; Iga, S.; Nasuno, T. Development of a global cloud resolving model – a multi-scale structure of tropical convections. J. Earth Simulator 2005, 3, 11–19.
27. GRABOWSKI, W.W. Toward Cloud Resolving Modeling of Large-Scale Tropical Circulations : A Simple Cloud Microphysics Parameterization. Am. Meteorol. Soc. 1998, 55, 3283–3298.
28. Skamarock, W.C.; Klemp, J.B.; Dudhi, J.; Gill, D.O.; Barker, D.M.; Duda, M.G.; Huang, X.-Y.; Wang, W.; Powers, J.G. A Description of the Advanced Research WRF Version 3. Tech. Rep. 2008, 113, doi:10.5065/D6DZ069T.
29. Grell, G.A.; Peckham, S.E.; Schmitz, R.; Mckeen, S.A.; Frost, G.; Skamarock, W.C.; Eder, B. Fully coupled '" online "' chemistry within the WRF model. Atmos. Environ. 2005, 39, 6957–6975, doi:10.1016/j.atmosenv.2005.04.027.
30. Janssens-Maenhout, G.; Pagliari, V.; Guizzardi, D.; Muntean, M. Global emission inventories in the Emission Database for Global Atmospheric Research (EDGAR) – Manual (I): Gridding: EDGAR emissions distribution on global gridmaps; 2013; ISBN 9789279282836.
31. Kumar, R.; Barth, M.C.; Pfister, G.G.; Nair, V.S.; Ghude, S.D.; Ojha, N. What controls the seasonal cycle of black carbon aerosols in India? J. Geophys. Res. 2015, 7788–7812, doi:10.1002/2015JD023298.
32. Wiedinmyer, C.; Akagi, S.K.; Yokelson, R.J.; Emmons, L.K.; Al-Saadi, J.A.; Orlando, J.J.; Soja, A.J. The Fire INventory from NCAR (FINN): A high resolution global model to estimate the emissions from open burning. Geosci. Model Dev. 2011, 4, 625–641, doi:10.5194/gmd-4-625-2011.
33. Emmons, L.K.; Walters, S.; Hess, P.G.; Lamarque, J.-F.F.; Pfister, G.G.; Fillmore, D.; Granier, C.; Guenther, A.; Kinnison, D.; Laepple, T.; et al. Description and evaluation of the Model for Ozone and Related chemical Tracers, version 4 (MOZART-4). Geosci. Model Dev. 2010, 3, 43–67, doi:10.5194/gmd-3-43-2010.
34. Mishra, A.; Srinivasan, J. Did a cloud burst occur in Kedarnath during 16 and 17 June 2013? Curr. Sci. 2013, 16–18.
35. Li, J.; Huang, H.-L.; Liu, C.-Y.; Yang, P.; Schmit, T.J.; Wei, H.; Weisz, E.; Guan, L.; Menzel, W.P. Retrieval of Cloud Microphysical Properties from MODIS and AIRS. J. Appl. Meteorol. 2005, 44, 1526–1543, doi:10.1175/jam2281.1.
36. Singh, P.; Adhikary, B.; Sarawade, P. Transport of black carbon from planetary boundary layer to free troposphere on a seasonal scale over South Asia. Atmos. Res. 2020, 235, 104761, doi:10.1016/j.atmosres.2019.104761.
37. Tajbakhsh, S.; Ghafarian, P.; Sahraian, F. Instability indices and forecasting thunderstorms: The case of 30 April 2009. Nat. Hazards Earth Syst. Sci. 2012, 12, 403–413, doi:10.5194/nhess-12-403-2012.
38. Singh, P. Prediction of Potential Thunderstorm Over Ocean near Sriharikota. Int. J. Interdiscip. Res. Innov. 2015, 3, 1–6.

39. Kain, J.S. The Kain–Fritsch Convective Parameterization: An Update. J. Appl. Meteorol. 2004, 43, 170–181, doi:10.1175/1520-0450(2004)043<0170:TKCPAU>2.0.CO;2.
40. Hong, S.-Y.; Noh, Y.; Dudhia, J. A New Vertical Diffusion Package with an Explicit Treatment of Entrainment Processes. Mon. Weather Rev. 2006, 134, 2318–2341, doi:10.1175/MWR3199.1.
41. Dudhia, J. Numerical Study of Convection Observed during the Winter Monsoon Experiment Using a Mesoscale Two-Dimensional Model. J. Atmos. Sci. 1989, 46, 3077–3107.
42. Thompson, G.; Field, P.R.; Rasmussen, R.M.; Hall, W.D. Explicit Forecasts of Winter Precipitation Using an Improved Bulk Microphysics Scheme. Part II: Implementation of a New Snow Parameterization. Mon. Weather Rev. 2008, 136, 5095–5115, doi:10.1175/2008MWR2387.1.
43. Mlawer, E.J.; Taubman, S.J.; Brown, P.D.; Iacono, M.J.; Clough, S.A. Radiative transfer for inhomogeneous atmospheres: RRTM, a validated correlated-k model for the longwave. J. Geophys. Res. Atmos. 1997, 102, 16663–16682, doi:10.1029/97JD00237.
44. Tewari, M.; Chen, F.; Wang, W.; Dudhia, J.; LeMone, M.A.; Mitchell, K.; Ek, M.; Gayno, G.; Wegiel, J.; Cuenca, R.H. Implementation and verification of the unified noah land surface model in the WRF model. Bull. Am. Meteorol. Soc. 2004, 2165–2170, doi:10.1007/s11269-013-0452-7.
45. Paulson, C.A. The Mathematical Representation of Wind Speed and Temperature Profiles in the Unstable Atmospheric Surface Layer. J. Appl. Meteorol. 1970, 9, 857–861.
46. Madronich, S.; Weller, G. Numerical integration errors in calculated tropospheric photodissociation rate coefficients. J. Atmos. Chem. 1990, 10, 289–300, doi:10.1007/BF00053864.